Non-radiative decay and stability of *N*-heterocyclic carbene iridium(III) complexes

Xiuwen Zhou[*], Benjamin J. Powell

School of Mathematics and Physics, The University of Queensland, Brisbane, Queensland 4072, Australia

ABSTRACT

Devices based on deep-blue emitting iridium (III) complexes with *N*-heterocyclic carbene (NHC) ligands have recently been shown to give excellent performance as phosphorescent organic light-emitting diodes (PHOLEDs). To facilitate the design of even better deep-blue phosphorescent emitters we carried out density functional theory (DFT) calculations of the lowest triplet (T_1) potential-energy surfaces (PES) upon lengthening the iridium-ligand (Ir-C) bonds. Relativistic time dependent DFT (TDDFT) calculations demonstrate that this changes the nature of T_1 from a highly-emissive metal-to-ligand charge transfer (^{3}MLCT) state to a metal centered (^{3}MC) state where the radiative decay rate is orders of magnitude slower than that of the ^{3}MLCT state. We identify the elongation of an Ir-C bond on the NHC group as the pathway with lowest energy barrier between the ^{3}MLCT and ^{3}MC states for all complexes studied and show that the barrier height is correlated with the experimentally measured non-radiative decay rate. This suggests that the thermal population of ^{3}MC states is the dominant non-radiative decay mechanism at room temperature. We show that the ^{3}MLCT -> ^{3}MC transition is reversible, in marked contrast to deep blue phosphors containing coordinating nitrogen atoms, where the population of ^{3}MC states breaks Ir-N bonds. This suggests that, as well as improved efficiency, blue PHOLEDs containing phosphors where the metal is only coordinated by carbon atoms will have improved device lifetimes.

INTRODUCTION

A major challenge in the field of phosphorescent organic light-emitting diode (PHOLED) technology is the lack of highly efficient emitters for saturated blue and deep-blue color to meet the demand of high quality displays.[1] Extensive efforts to develop blue phosphorescent iridium(III) [Ir(III)] complexes have been motivated by the existing highly efficient green and red Ir(III) phosphors, especially the green emitter *fac*-tris(2-phenyl-pyridyl)iridium(III) [Ir(ppy)$_3$],[2] which displays a near unity photoluminescence quantum yield (PLQY). However, there are still only a small number of known blue phosphorescent Ir(III) complexes. Furthermore, most of these emit sky-blue light, which is inadequate for full color displays and lighting applications. The known deep blue emitters suffer from relatively low PLQY and stability issues in devices.[1]

Ligand modification of existing emitters is often used to tune the color of Ir(III) complexes,

1

however it also often dramatically changes the room-temperature PLQY; many times from near 1 to near 0.[3-5] The dramatic decrease in PLQY is primarily[3, 6] due to the increase in non-radiative rate of the emissive state (typically from ~10^3 s^{-1} to >10^8 s^{-1}), with the radiative rate remaining of the order of 10^5 s^{-1} for the most promising deep blue emitters.[3, 6] Therefore, in order to predict the PLQY of Ir(III) complex, the key theoretical challenge is to understand the non-radiative decay processes of the emissive state. A number of non-radiative processes have been discussed including: intramolecular vibronic coupling quenching[7, 8], thermal population to non-radiative states[6, 9, 10], intermolecular quenching[11, 12].

The quantum efficiency can be expressed as a function of radiative and non-radiative rates by[13],

$$\Phi_{PL} = \frac{k_r}{k_r + k_{nr}}, \tag{1}$$

where Φ_{PL} is the PLQY, k_r is the radiative rate, and k_{nr} is the non-radiative rate. Different non-radiative decay mechanisms lead to dramatically different temperature dependences of k_{nr}. For example, k_{nr} due to vibronic coupling is largely temperature independent, whereas the rate due to the thermal population to an upper level non-radiative state (which cannot decay radiatively or does so only very slowly) is highly temperature dependent. This non-radiative process would lead to an activated behavior, hence the rate can be expressed in terms of the Arrhenius equation[14],

$$k_{nr}(T) = k_a e^{-\Delta E/k_B T}, \tag{2}$$

where k_a is the rate constant, ΔE is the activation energy to the upper level, and k_B is the Boltzmann constant. The exponential decrease in $k_{nr}(T)$ as ΔE increases implies that small differences in the activation energies change $k_{nr}(T)$ dramatically. Several authors[6, 9, 15-19, 10] have argued that the thermal population of non-radiative metal-centered (^{3}MC or ^{3}dd*) states is the dominant non-radiative decay mechanism in blue phosphorescent Ir(III) complexes at room temperature. Since the transitions from these ^{3}MC states to the ground state have strong metal-to-metal (d* -> d) character they provide little possibility of radiative decay. This is consistent with the experimental observation that k_{nr}, and hence the PLQY, is clearly temperature dependent, i.e., at low-temperature k_{nr} is very slow (PLQY is very high) for many complexes while on increasing the temperature towards room temperature k_{nr} (PLQY) increases (decreases) dramatically[6].

Recently, we have shown[19] that there are only small energy barriers (relative to $k_B T$) between the emissive metal-to-ligand charge transfer (^{3}MLCT) states and non-radiative ^{3}MC states in a family of Ir(III) complexes based on *fac*-tris(1-methyl-5-phenyl-3-*n*-propyl-[1,2,4]triazolyl)iridium(III) [Ir(ptz)$_3$]. The lowest energy barrier path to non-radiative states for these complexes is the elongation of an Ir-N bond. The calculated barrier energy correlates with the experimental non-radiative rate, as expected from Eq. (2). Importantly, once the non-radiative states were formed, the complexes were not able to return to the emissive states, resulting in permanent damage to the structure via breaking of the Ir-N bond. This explains the poor stability of PHOLED devices based on them. These findings and the applied theoretical methods have been used to predict Ir(III) complexes with higher PLQY in the design of new complexes based on Ir(ptz)$_3$.[10]

Recently, deep-blue-emitting PHOLEDs based on tris-(*N*-phenyl,*N*-methyl-pyridoimidazol-2-yl)iridium(III), Ir(pmp)$_3$ (see right panels of Figure 1) achieved the brightest deep blue emission

among the PHOLEDs reported. Indeed, devices based on its facial isomer [*fac*-Ir(pmp)₃] perform close to the most stringent US National Television System Committee requirements.[20] The meridional isomer (*mer*-Ir(pmp)₃) was also found equally efficiently luminescent; the PLQYs of the two isomers are equal within the reported errors, cf. Table 3. However, both isomers of the closely related tris-(*N*-phenyl, *N*-methyl-benzimidazol-2-yl) Ir(III), Ir(pmb)₃ (see left panels in Figure 1) have much lower luminescence efficiency at room temperature, in fact *mer*-Ir(pmb)₃ is barely luminescent[21] (the experimental PLQYs are reproduced in Table 3). In order to further design new blue Ir(III) complexes based on NHC ligands suitable as emitters in PHOLEDs, it is very important to understand the non-radiative pathways and stability of these complexes, and why apparently small chemical changes so dramatically alter their photophysical properties.

As a first step towards these goals, here we investigate the possible reaction paths to non-radiative states for these four complexes and the correlation between the lowest activation barrier to non-radiative states and the experimental non-radiative rate. We also discuss how ligand substitution and structural isomerization affect the photoluminescence efficiency and the stability of these complexes. We show that the barriers between the ^{3}MLCT and ^{3}MC excited states are large for both isomers of the Ir(pmp)₃ complex, consistent with their high PLQYs, and smaller in Ir(pmp)₃. Furthermore we find that, unlike in other blue phosphorescent complexes, when the material reaches the ^{3}MC state this does *not* break the stretched metal-ligand bond. This allows for the possibility of complex returning to the emissive ^{3}MLCT state, further increasing the PLQY of these complexes. It also means that excitations of the ^{3}MC state do not cause permanent damage to the complex – this suggests that PHOLEDs based on Ir(pmp)₃ should have much better device lifetimes than those for PHOLEDs with other blue phosphorescent active materials.
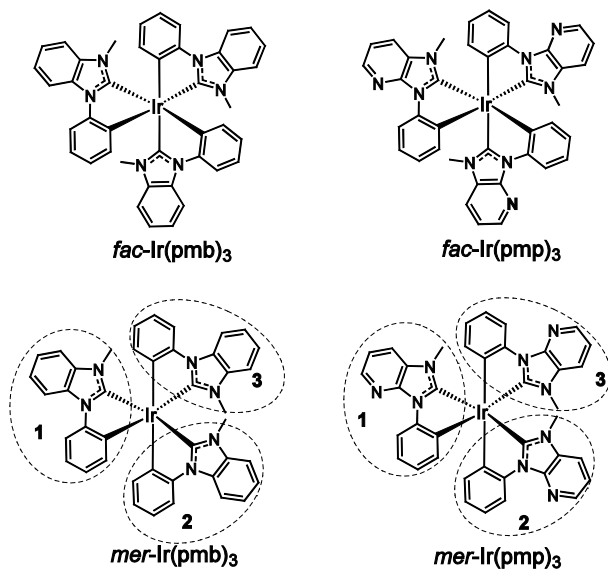

fac-Ir(pmb)₃   *fac*-Ir(pmp)₃

mer-Ir(pmb)₃   *mer*-Ir(pmp)₃

Figure 1. Structures of the facial (*fac*-) and meridional (*mer*-) isomers of Ir(pmb)₃ and Ir(pmp)₃. These are closely related complexes – a methine replaced by a nitrogen atom in the NHC ligands (CH -> N) from pmb to pmp. This modification not only redshifts the emission from near ultraviolet to the deep blue region, but also greatly increases the PLQY (see Table 3). The ligands of *mer*-isomers are numbered to distinguish the six inequivalent Ir-ligand bonds.

CALCULATIONS

Geometry

The structures of *fac-* and *mer*-Ir(pmb)$_3$ were optimized taking the measured crystal structures[21] as starting points. The structures of *fac-* and *mer*-Ir(pmp)$_3$ were then optimized with the initial structures based on the optimized structures of *fac-* and *mer*-Ir(pmb)$_3$, respectively. The geometry optimization was performed with density functional theory (DFT)[22, 23] using the B3LYP[24, 25] functional. The 6-31G(d,p) basis set[26] was used for hydrogen, carbon, and nitrogen, and the LANL2DZ basis set[27] with an effective core (Los Alamos ECP[27]) was used for iridium. All calculations in this work except those of the radiative rate and electronic excitations were performed using the Gaussian 09 set of programs[28], with the functional and basis set described above used throughout. All calculations were performed for molecules in gas phase.

Triplet potential-energy surface

Several previous studies[9, 15, 6, 19] indicate that for emissive cyclometalated complexes the reaction path to non-radiative states is the elongation or even breaking of a metal-ligand bond. To find the lowest-energy-barrier reaction path to non-radiative states, we therefore performed a relaxed potential-energy surface (PES) scan for the emissive state, that is, the lowest energy triplet (T$_1$) state, along the reaction path of the elongation of each inequivalent Ir-C bond. Note that, for the two *fac*-isomers (upper panels of Figure 1), each complex has two types of inequivalent Ir-ligand bonds, i.e., three equivalent Ir-C (NHC) bonds and three equivalent Ir-C (PHE) bonds, where PHE denotes phenyl and the label in brackets indicates the group containing the relevant carbon atom. However, for the two *mer*-isomers (lower panels of Figure 1), all six Ir-ligand bonds are unique. To distinguish these six bonds, we label the three ligands 1-3 (Figure 1).

In the relaxed PES scan, the starting structure had the Ir-C bond length equal to that found in the optimized ground-state structure. This bond was then lengthened in 0.1 Å increments. The geometry at each point along this path was optimized subject to the length constraint on this single extended bond. The initial geometry for each optimization after increasing the Ir-C bond length took the position of the remaining atoms to be those found in optimized structure for the previous Ir-C bond length. The energy of the T$_1$ state was then calculated. Unrestricted DFT was used for treating the T$_1$ states since they contain unpaired electrons, which is known[29] to be quite good at modelling the properties of open-shell molecular systems including spin polarization (in contrast, the unrestricted Hartree-Fock approximation overestimates polarization) and energetics. To optimize the triplet states and calculate the triplet energies, a quadratically convergent self-consistent field (SCF) procedure[30] was used that is slower than regular SCF but more reliable.

Radiative rate and low-energy excitations

Relativistic calculations were performed for selected structures to obtain the radiative rate and more accurate information on electron excitations. In these calculations, spin-orbit coupling (SOC) was added perturbatively[31] to one-component TDDFT[32-34] utilizing the one-component zeroth order regular approximation (ZORA).[35, 36] A total of 40 spin-mixed excitations were calculated. The radiative rate (k_r) of an excited state was then calculated according to[37-39]

$$k_r = 2\epsilon^2 f/c^3, \tag{3}$$

4

where ϵ is the excitation energy and f is the corresponding oscillate strength for the electronic excitation from the ground state to the excited state. The three lowest energy states found in the SOC TDDFT calculations for the complexes considered here are derived from the three substates in a triplet state with a small singlet admixture due to SOC[40, 41]. There will be small energy differences between the three states because of their different admixtures with the singlet state, the so called zero-field splitting (ZFS). As the ZFS is small compared to k_BT at room temperature, the radiative rate of the triplet state is then calculated as an average over the three substates within the assumption of fast thermalization.

The calculations were carried out with ADF (2017 version),[39] using the B3LYP[24, 25] functional and Slater type TZP basis sets[42, 43]. The B3LYP functional was chosen since many of the low-energy excitations of the complexes studied here have metal-to-ligand charge transfer character. It is well known[44-47] that the inclusion of Hartree-Fock exact exchange significantly improves the physical description of charge-transfer excited states of small molecules in the TDDFT calculations. Extensive benchmarking[48] has shown that B3LYP accurately reproduces the energetics of these Ir(III) complexes.[40]

RESULTS & DISCUSSION

Optimized geometries and the concomitant electronic structure

To understand the impact of isomerization and CH -> N substitution on the ligand in the ground-state geometry, key geometric parameters (length of six Ir-ligand bonds) are collated in Table 1. The ligand substitution causes negligible change in the length of the six Ir-ligand bonds; all bond lengths are almost identical for Ir(pmb)$_3$ and Ir(pmp)$_3$. *Fac*-isomers have equal lengths for all Ir-C (NHC) bonds and all Ir-C (PHE) bonds due to their C$_3$ symmetry. The Ir-C (NHC) bonds are 0.05 Å shorter than the Ir-C (PHE) bonds. However, *mer*-isomers have different lengths for all six Ir-ligand bonds due to its asymmetric molecular structure (C$_1$). Table 1 indicates an Ir-C (PHE) bond is the weakest bond in ground state if one naïvely expects that the greater bond length of a covalent bond has the weaker the bond is. Our interest is to find the weakest Ir-C bond in excited state thus the lowest energy barrier pathway from the ^{3}MLCT state to the ^{3}MC state. We will see below, that for both facial isomers the shorter NHC bonds provide a lower energy barrier pathway and that in both meridional complexes the elongation of the Ir-C (NHC) bond that is longest in the ground state geometry, i.e., Ir-C (NHC$_3$), has the lowest barrier between the ^{3}MLCT and ^{3}MC states. Therefore, no direct correlation is found between the ground-state bond lengths with the strength of the bonds in excited state.

Table 1. Bond lengths (six Ir-C bonds) of *fac*- and *mer*- isomers of Ir(pmb)$_3$ and Ir(pmp)$_3$ at geometries optimized for ground state. *Fac*-isomers have two inequivalent types of metal-ligand bonds, i.e., Ir-C (NHC) bonds and Ir-C (PHE), while *mer*-isomers have six inequivalent bonds, the indices 1, 2, and 3 denote the ligand containing that bond (cf. Figure 1).

complex	Ir-C (NHC$_1$)	Ir-C (PHE$_1$)	Ir-C (NHC$_2$)	Ir-C (PHE$_2$)	Ir-C (NHC$_3$)	Ir-C (PHE$_3$)
fac-Ir(pmb)$_3$	2.06	2.11	2.06	2.11	2.06	2.11

fac-Ir(pmp)$_3$	2.06	2.11	2.06	2.11	2.06	2.11
mer-Ir(pmb)$_3$	2.06	2.09	2.05	2.12	2.08	2.14
mer-Ir(pmp)$_3$	2.06	2.10	2.05	2.12	2.08	2.14

It has been previously shown that the lowest excitation of cyclometalated phosphors is predominately a highest occupied molecular orbital (HOMO) to lowest unoccupied molecular orbital (LUMO) transition and their T$_1$ states have strong MLCT character.[49, 40, 19] The NHC Ir(III) complexes studied here also have a lowest excitation that is predominantly a HOMO->LUMO transition (~ 60% weight). From the frontier molecular orbitals shown in Figure 2, the HOMO of *fac*-isomer is distributed mainly on the metal atom and the three phenyl rings, whereas its LUMO is distributed mainly on the NHC ligands. For the *mer*-isomer, the HOMO is mainly distributed on the metal and two of three phenyl rings (ligands 1 and 2; cf. Figure 1), while the LUMO is distributed mainly on the NHC part of ligand 3. This suggests that, in their optimized ground state geometries, the T$_1$ states of both isomers have both metal-to-ligand change transfer character and ligand-to-ligand change transfer character. This charge redistribution is crucial for understand the bond strengths in the excited states.
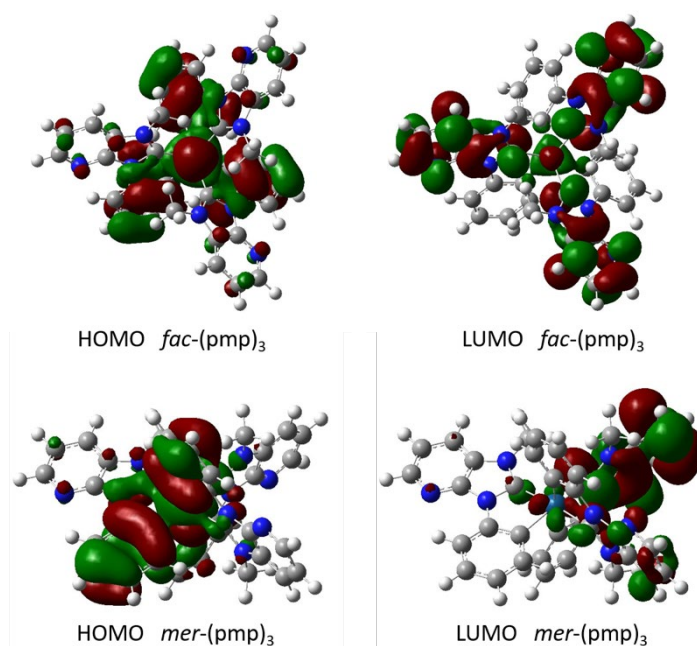

HOMO *fac*-(pmp)$_3$ LUMO *fac*-(pmp)$_3$

HOMO *mer*-(pmp)$_3$ LUMO *mer*-(pmp)$_3$

Figure 2. Frontier molecular orbitals (HOMO and LUMO) of *fac*- and *mer*-Ir(pmp)$_3$ in their optimized ground state geometries. The equivalent orbitals for *fac*- and *mer*-Ir(pmb)$_3$ show the same trend (cf. Figure S1), i.e., a significant metallic contribution to the HOMO but not the LUMO.

Non-radiative decay paths and characterization of T$_1$ states

The calculated PES curves for the T$_1$ state under the elongation of each inequivalent Ir-ligand (Ir-C) bond are shown in Figure 3. As the bond is elongated most curves show an initial arise and then a drop to a flatter region after reaching a maximum energy, although for a few bonds the energy continues to increase as the bond length increases for throughout the range studied. The states on

6

the right-hand-side of the barriers (i.e., at the local minima for elongated bonds) are ^{3}MC states (i.e., the spin density of these states shows a heavy contribution from the metal, cf. Figure S2). Thus, we will see below that, the metal-ligand bond stretches are non-radiative decay paths and that the T_1 state becomes dramatically less radiative as the bond is elongated.

For both *fac*-isomers, the lowest barrier non-radiative path is the elongation of an Ir-C (NHC) bond rather than an Ir-C (PHE) bond, see Figure 3. Thus, *in the excited state* the Ir-C (NHC) bonds are weaker than the Ir-C (PHE) bonds. This can be understood as a consequence of the charge transferred from PHE into the NHC group in the excited state (cf. HOMO and LUMO in Figure 1). The HOMO is comprised by a metal d orbital and π^* antibonding orbitals located on PHE part of the ligand. However, the LUMO has the π^* antibonding orbitals located on NHC part of the ligand. This would lead to a weakened Ir-C (NHC) bond in excited state.

For both *mer*-isomers, the lowest-energy-barrier non-radiative path is the elongation of the Ir-C (NHC) bond in ligand 3 (cf. Figure 1), which is the longest, and thus presumably the weakest, Ir-C (NHC) bond in the ground state geometry. Interestingly, the π^* antibonding orbitals of the LUMO of *mer*-isomers are also mainly distributed on the NHC part of ligand 3. This is consistent with the idea that the electron transfer from the metal and phenyl rings to this NHC part facilitates the elongation of this bond.
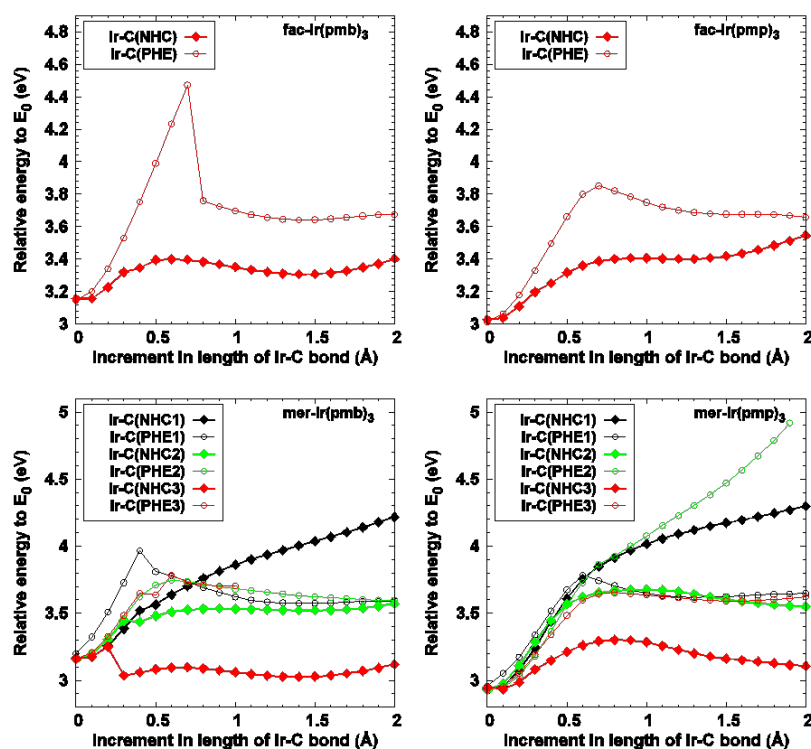

Figure 3. PESs of *fac*- and *mer*-Ir(pmp)$_3$ and *fac*- and *mer*-Ir(pmp)$_3$ as an Ir-C bond is lengthened and the remaining atomic positions are optimized self-consistently. All curves show the energy of the T_1 state when the geometry is optimized for the T_1 state. Here E_0 is the singlet energy of the singlet ground-state geometry. See Figure 1 for the definition of the ligand numbering.

The character of the T_1 states along the reaction paths is analyzed through the calculation of radiative rate (from the three substates of T_1 to the singlet ground state S_0), excitation energy and oscillator strengths of the lowest three spin-mixed excitations, and the spin density. This allows the identification of non-radiative states that have small radiative rate thus small possibility to decay

7

radiatively. To facilitate this analysis we report detailed calculations for the T_1 states at four key points on the lowest barrier path of each complex. The key T_1 states are: the Frank-Condon state (in ground-state geometry), the optimized ^{3}MLCT state (relaxed from the Frank-Condon state), an intermediate ^{3}MC (non-radiative) state extracted from the T_1 PES, and the optimized ^{3}MC state (relaxed from an intermediate ^{3}MC state). These states are identified in Figure 4 and denoted in Figure 5.

The calculated results for average radiative rate, excitation energy and oscillator strengths from the lowest three spin-mixed excitations are collated in Table 2. The T_1 states become less radiative and eventually reach a dark state (such as the optimized ^{3}MC state) with the radiative rate equal or close to zero. Furthermore, the S_0-T_1 excitation energy decreases and eventually T_1 state becomes the ground electronic state in the studied geometries (for clarity we do not alter the names of the states when this happens). Indeed this is the case at the optimized ^{3}MC states of two meridional complexes and fac-Ir(pmb)$_3$. Note that the radiative rates of the intermediate ^{3}MC states ($\sim 10^2$ s^{-1}) are 2-3 orders of magnitudes slower than that of the respective emissive (^{3}MLCT) states ($\sim 10^5$ s^{-1}). The intermediate ^{3}MC states have very low excitation energies (< 1 eV) and small oscillator strengths ($\sim 10^{-5}$). This indicates that the intermediate ^{3}MC states already have little probability to decay radiatively. This is important because it suggests that thermal excitations about the very shallow ^{3}MC minimum do not allow for significant radiative decay and that the ^{3}MC states remain dark when such vibrations are excited.
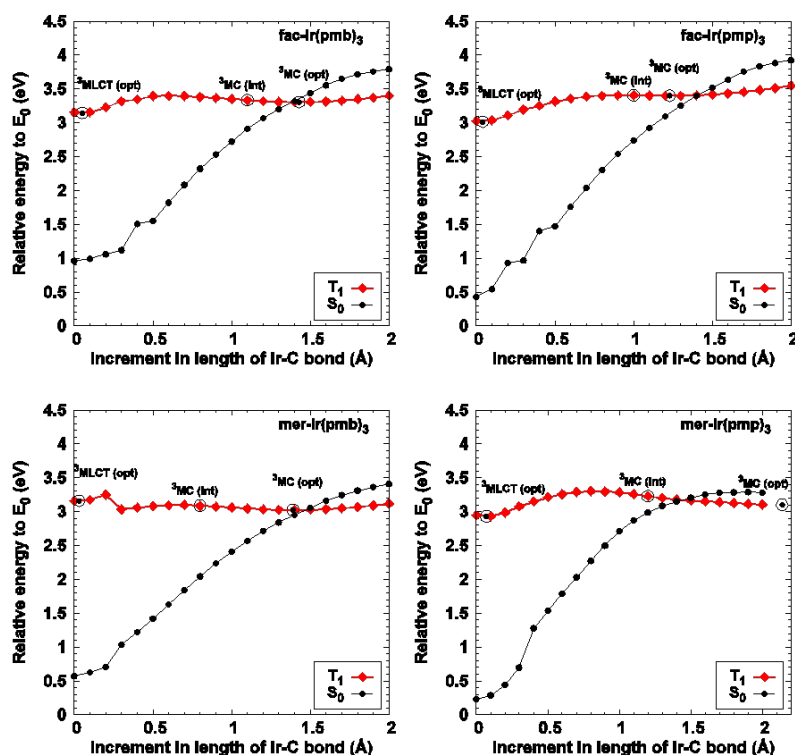

Figure 4. PESs of fac- and mer-Ir(pmp)$_3$ and fac- and mer-Ir(pmp)$_3$. The "T_1" curves (red) are the lowest barrier path to non-radiative states in Figure 3, showing the energy of the T_1 state when the geometry is optimized for the T_1 state. While the "S_0" curves (black) show the energy of the lowest energy singlet state in the geometry optimized for the T_1 state. The optimized ^{3}MLCT state, an intermediate ^{3}MC state on the T_1 PES from where the ^{3}MC state is optimized, and the optimized ^{3}MC state are marked on the "T_1" curves. Here E_0 is the singlet energy of the singlet ground-state geometry.

Table 2. Calculated average excitation energies (ε) and corresponding oscillator strengths (f), and radiative rates (k_r) of the three substates of T_1 states.[a]

complex	State[b]	ε (eV)[c]	f	k_r (s^{-1})
fac-Ir(pmb)$_3$	^{3}MLCT (Frank-Condon)	3.31	2×10^{-4}	9×10^4
	^{3}MLCT (optimized)	2.05	1×10^{-4}	3×10^4
	^{3}MC (intermediate)	0.11	3×10^{-5}	2
	^{3}MC (optimized)	-0.17	1×10^{-5}	0
fac-Ir(pmp)$_3$	^{3}MLCT (Frank-Condon)	2.98	3×10^{-4}	1×10^5
	^{3}MLCT (optimized)	2.34	1×10^{-4}	3×10^4
	^{3}MC (intermediate)	0.37	2×10^{-5}	1×10^2
	^{3}MC (optimized)	0.02	7×10^{-5}	1
mer-Ir(pmb)$_3$	^{3}MLCT (Frank-Condon)	3.23	2×10^{-4}	8×10^4
	^{3}MLCT (optimized)	2.44	1×10^{-4}	3×10^4
	^{3}MC (intermediate)	0.97	1×10^{-5}	5×10^2
	^{3}MC (optimized)	-0.16	2×10^{-5}	0
mer-Ir(pmp)$_3$	^{3}MLCT (Frank-Condon)	2.84	1×10^{-4}	5×10^4
	^{3}MLCT (optimized)	2.38	3×10^{-5}	9×10^3
	^{3}MC (intermediate)	0.15	1×10^{-5}	9
	^{3}MC (optimized)	-0.07	7×10^{-6}	0

[a] The lowest three spin-mixed excitations (i.e. S_0 to the three substates of T_1) are considered. The radiative rate is calculated for the substates of T_1 decaying to the singlet ground state.
[b] Here ^{3}MLCT (Frank-Condon) denotes the T_1 state in ground-state geometry, ^{3}MLCT (optimized) denotes the optimized T_1 state started from the ground-state geometry, ^{3}MC (intermediate) denotes a prototype non-radiative state on T_1 PES in Figure 4, and ^{3}MC (optimized) denotes the optimized T_1 state started from the ^{3}MC (intermediate) geometry.
[c] The respective S_0-T_1 electronic excitations are sketched in Figure 5. Negative values indicate a triplet ground state.

Figure 5. Schematic representation of the PESs of the T_1 states and the relevant lowest-energy singlet state (S_0) of NHC Ir(III) complexes. The S_0-T_1 excitations for the T_1 states in Table 2 are marked by arrows.

1. ^{3}MLCT(Frank-Condon)
2. ^{3}MLCT (optimized)
3. ^{3}MC (intermediate)
4. ^{3}MC (optimized)
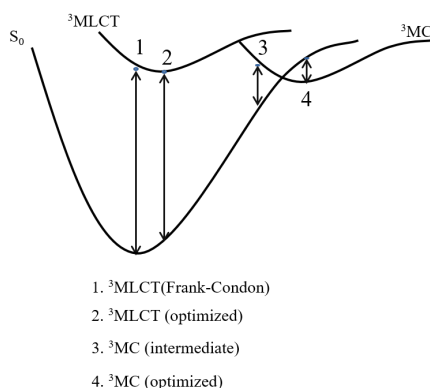
Impact of CH->N ligand substitution and structural isomerization on PLQY

The lowest energy barriers to non-radiative states for all four complexes are tabulated in Table 3. A simple relationship is found between the activation barrier and the non-radiative rate of the four complexes: the larger the barrier, the lower the non-radiative rate. Clearly this is consistent with decay via a ^{3}MC state being the dominant non-radiative decay pathway at room temperature for these NHC Ir(III) complexes (see Equations 1 and 2).

To understand the impact of the ligand substitution CH->N (i.e., pmb -> pmp) on the luminescence efficiency, let us take a closer look at the energy barriers to the non-radiative states and the shape of PES from emissive states to non-radiative states. From *fac*-Ir(pmb)$_3$ to *fac*-Ir(pmp)$_3$, the energy barrier to non-radiative rate increases from 0.24 eV to 0.38 eV, this causes the non-radiative decay rate to decrease by an order of magnitude. However, the radiative rates (both calculated and measured) of two complexes are in the same order of magnitude. Therefore the overall PLQY is increased by the ligand substitution (CH->N). Moreover, the energy barrier from non-radiative state back to emissive state is lowered (cf. Figure 6), which indicates that the ligand substitution also leads to less stable non-radiative states.

A similar but even higher impact of ligand substitution can be observed from *mer*-Ir(pmb)$_3$ to *mer*-Ir(pmp)$_3$ -- the energy barrier to the non-radiative state increases from 0.09 eV to 0.35 eV, and the non-radiative state of *mer*-Ir(pmb)$_3$ is more stable than its emissive state (lower T_1 energy in the non-radiative state)! This explains why *mer*-Ir(pmb)$_3$ is nearly non-emissive at room temperature (with a very low PLQY of 0.2). The impact of CH->N substitution on k_{nr} might be due to the greater electronegativity of the N atom than the CH group strengthening the Ir-C (NHC) bond and thus lifting the energy barrier to non-radiative states and resulting a slower k_{nr}.

The impact of isomerization (from facial to meridional) on PLQY is however less significant than that of CH->N substitution. Overall the *fac*-isomers have higher energy barriers to the non-radiative rate states and thus smaller k_{nr}, although the difference between *fac*-Ir(pmp)$_3$, and *mer*-Ir(pmp)$_3$ is very small (the energy barrier former in the is 0.03 eV greater). The lowered symmetry (from C_3 to C_1) allows the weakening of one of the Ir-C (NHC) bonds and thus decreases the energy barrier to non-radiative rate and increases the k_{nr}. As the weakest bond determines the non-radiative decay rate any strengthening of the other bonds does not compensate for this.

Table 3. Calculated activation energy to the ^{3}MC states (ΔE), non-radiative rate at 295 K divided by the rate constant $(k_{nr}[295K]/k_a$, see Equation 2), radiative rate at 0 K $(k_r[0K])$, and emission energy (λ_{max}) of four NHC Ir(III) complexes. The measured room-temperature non-radiative rates (k_{nr}), radiative rates (k_r), photoluminescent quantum yields (Φ_{PL}), and emission peak wavelengths (λ_{max}) are also given for comparison.

| complex | calculated | | | | experimental | | | | |
	ΔE (eV)	$k_{nr}[295K]/k_a$	$k_r[0K]$ (s^{-1})	λ_{max} (nm)*	$k_{nr}[295K]$ (s^{-1})	$k_r[295K]$ (s^{-1})	Φ_{PL} (%) [295K]	λ_{max} (nm)	Ref.
fac-Ir(pmb)$_3$	0.24	6.8×10^{-5}	0.9×10^5	375	5.7×10^5	3.4×10^5	37	-	6
					4.0×10^6	1.8×10^5	4	380	21

fac-Ir(pmp)$_3$	0.38	3.6×10^{-7}	1.0×10^5	416	$(2.0\pm0.4)\times10^5$	$(6.4\pm1.3)\times10^5$	76±5	418	[20]
mer-Ir(pmb)$_3$	0.09	3.1×10^{-2}	0.8×10^5	384	6.50×10^7	1.3×10^5	0.2	385	[21]
mer-Ir(pmp)$_3$	0.35	9.7×10^{-7}	0.5×10^5	437	$(2.7\pm0.4)\times10^5$	$(10\pm2)\times10^5$	78±5	465	[20]

[*] Emission wavelengths are converted from the excitation energy values of the Frank-Condon states in Table 2.

Stability of NHC Ir(III) complexes

To understand the stability of the molecules in the ^{3}MC state we investigated how the energetics of T$_1$ state and molecular structures change when the Ir-C (NHC) bond is shorted starting from the ^{3}MC (int) state marked in Figure 4 for the lowest-energy-barrier non-radiative path identified above.

We find that the ^{3}MC states of all four complexes are able to return to a geometry very similar to the equilibrium one, i.e., have similar T$_1$ energies (see the initial points of the PESs in Figure 4) and metal-ligand bond lengths. This indicates that even these complexes are thermally populated to ^{3}MC states, they are still able to return to the ^{3}MLCT states. The Ir-C bond does not break! Thus, the thermal population to ^{3}MC states does not lead to a permanent damage to the structure of the Ir(pmp)$_3$ and Ir(pmb)$_3$ complexes, although it results in a dramatically decreased radiative rate. This is very different behavior from that found for complexes with Ir-N metal-ligand bonds[19, 10]. Ir(ptz)$_3$ and similar complexes are unable to return to the ^{3}MLCT state once the ^{3}MC state is formed. Instead shortening the relevant bond length results in another ^{3}MC state (one of other Ir-N bonds grows to more than 1 Å longer than the equilibrium ^{3}MLCT state), which has lower T$_1$ energy than the equilibrium ^{3}MLCT state! This indicates that the formation of ^{3}MC state in Ir(ptz)$_3$ based complexes leads to both an increased non-radiative rate and a permanent damage of the emitters in device. Figure 6 leads us to predict that all four complexes studied here should have good stability in devices under repeated use. Thus we expect that PHOLEDs with Ir(pmp)$_3$ as their active material should have good device lifetimes.
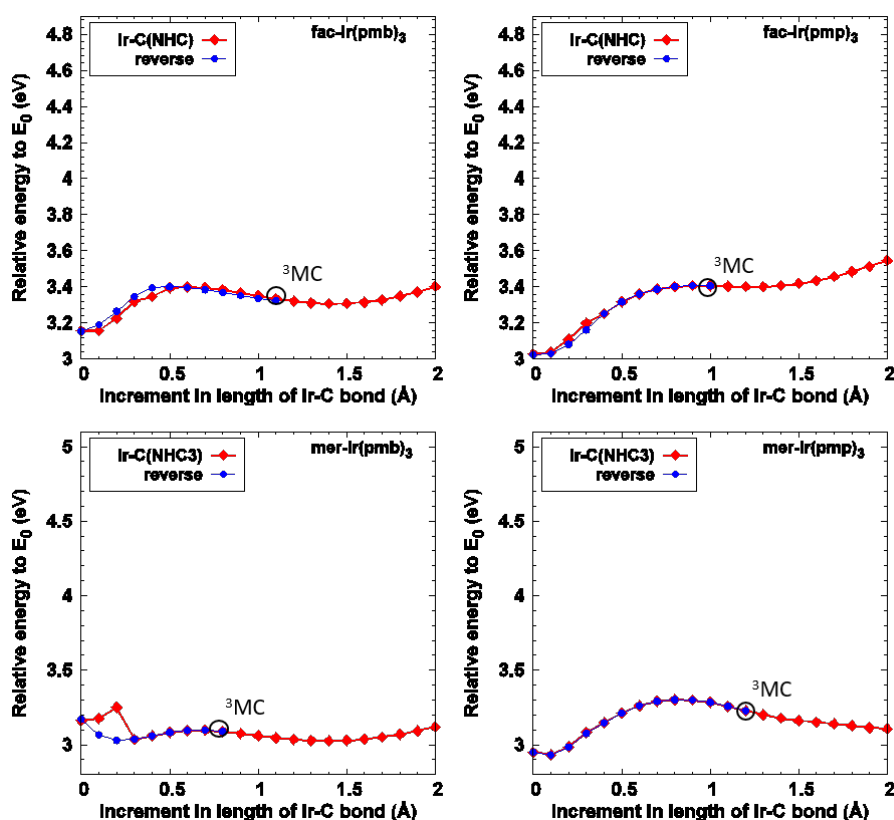
Figure 6. PESs of *fac-* and *mer-*Ir(pmp)₃ and *fac-* and *mer-*Ir(pmp)₃ as an Ir-C (NHC) bond is lengthened and the remaining atomic positions are optimized self-consistently. All curves show the energy of the T_1 state when the geometry is optimized for the T_1 state. The red diamonds denote a reaction path where an Ir-C (NHC) bond is elongated (i.e., moving from left to right) starting from the ³MLCT state along the lowest barrier path to ³MC state (cf. Figure 4), while the blue diamonds denote the reaction path on the shortening of an Ir-C (NHC) bond (i.e., moving from right to left) starting from an intermediate ³MC state marked in Figure 4.

CONCLUSIONS

We have demonstrated that the experimentally measured non-radiative decay rates in a family of *N*-heterocyclic carbene iridium(III) complexes are correlated with the energy barriers between ³MLCT and ³MC excited states. Furthermore, the calculated radiative decay rates of the latter are orders of magnitude slower than the calculated radiative decay rates of the former, which is consistent with the experimentally measured rates. This suggests that thermal population of the "dark" ³MC states is the dominant non-radiative decay mechanism. The T_1 PESs indicate that the elongation of an Ir-C (NHC) bond is the most likely path to the dark states for all four complexes discussed in this paper. It is interesting to contrast this with ground state structure, where the Ir-C (NHC) bonds are shorter than the Ir-C (PHE) bonds. However, the calculated frontier molecular orbitals suggest that there is significant charge transferred into the NHC moieties in the excited state. This appears to lead to the weakening of the Ir-C (NHC) bonds in the excited state.

CH->N ligand substitution stabilizes the Ir-C (NHC) bond in the excited state; lifting the activation barrier and hence suppressing the non-radiative rate. Isomerization from facial to meridional isomer

lowers the symmetry of the molecule, which weakens at least one Ir-C (NHC) bond and thus increases the non-radiative rate.

Finally, we found that the lengthening of the Ir-C (NHC) bond is reversible. This is in marked contrast to Ir(ptz)$_3$ and its fluorinated derivatives, which we studied previously[19, 10]. In these materials lengthening the Ir-N bond sufficiently to reach the ^{3}MC state is irreversible as it breaks the Ir-N bond. This indicates that the NHC Ir(III) complexes studied here are able to return to the ^{3}MLCT state from the ^{3}MC state. More importantly, the thermal population of complexes in the ^{3}MC state does not lead to permanent damage of the complexes in a device setting.

More generally it is interesting to speculate that the stability of the Ir-C bonds in ^{3}MC excited states may be significantly better than Ir-N bonds. It seems likely that, for example, the stability and efficiency of Ir(ppy)$_3$ could arise from a large barrier between the ^{3}MLCT and ^{3}MC states, rather than the properties of the ^{3}MC state itself. This suggests that exploring other complexes where all coordinating atoms are carbon, particularly other NHC ligands, may be a powerful strategy for improving both the efficiency and device lifetimes of deep blue PHOLEDs.

SUPPLEMENTARY MATERIAL

Supporting information and listings of the Cartesian coordinates of the optimized geometries of the four NHC Ir(III) complexes studied in this work.

ACKNOWLEDGMENTS

REFERENCES

(1)   X. Yang, X. Xu, and G. Zhou, "Recent advances of the emitters for high performance deep-blue organic light-emitting diodes," *J. Mater. Chem. C*, vol. 3, no. 5, pp. 913–944, 2015.

(2)   C. Adachi, M. A. Baldo, S. R. Forrest, and M. E. Thompson, "High-efficiency organic electrophosphorescent devices with tris(2-phenylpyridine)iridium doped into electron-transporting materials," *Appl. Phys. Lett.*, vol. 77, no. 6, p. 904, 2000.

(3)   S.-C. Lo, C. P. Shipley, R. N. Bera, R. E. Harding, A. R. Cowley, P. L. Burn, and I. D. W. Samuel, "Blue phosphorescence from iridium(III) complexes at room temperature," *Chem. Mater.*, vol. 18, no. 21, pp. 5119–5129, 2006.

(4)   Y.-S. Yeh, Y.-M. Cheng, P.-T. Chou, G.-H. Lee, C.-H. Yang, Y. Chi, C.-F. Shu, and C.-H. Wang, "A new family of homoleptic Ir(III) complexes: Tris-pyridyl azolate derivatives with dual phosphorescence," *ChemPhysChem*, vol. 7, no. 11, pp. 2294–2297, 2006.

(5)   A. C. Jacko, R. H. McKenzie, and B. J. Powell, "Models of organometallic complexes for optoelectronic applications," *J. Mater. Chem.*, vol. 20, no. 46, pp. 10301–10307, 2010.

(6)   T. Sajoto, P. I. Djurovich, A. B. Tamayo, J. Oxgaard, W. A. Goddard III, and M. E. Thompson, "Temperature dependence of blue phosphorescent cyclometalated Ir(III) complexes," *J. Am. Chem. Soc.*, vol. 131, no. 28, pp. 9813–9822, 2009.

(7)   J. V. Caspar, E. M. Kober, B. P. Sullivan, and T. J. Meyer, "Application of the energy gap law to the decay of charge-transfer excited states," *J. Am. Chem. Soc.*, vol. 104, no. 2, pp. 630–632, 1982.

(8)   R. E. Harding, S.-C. Lo, P. L. Burn, and I. D. W. Samuel, "Non-radiative decay mechanisms in blue phosphorescent iridium (III) complexes," *Org. Electron.*, vol. 9, no. 3, pp. 377–384, 2008.

(9)   G. Treboux, J. Mizukami, M. Yabe, and S. Nakamura, "Blue phosphorescent iridium(III) complex. A reaction path on the triplet potential energy surface," *Chem. Lett.*, vol. 36, no. 11, pp. 1344–1345, 2007.

(10)   X. Zhou, P. L. Burn, and B. J. Powell, "Effect of n-propyl substituents on the emission properties of blue phosphorescent iridium (iii) complexes," *J. Chem. Phys.*, vol. 146, no. 17, p. 174305, 2017.

(11)   S. Reineke, K. Walzer, and K. Leo, "Triplet-exciton quenching in organic phosphorescent light-emitting diodes with Ir-based emitters," *Phys. Rev. B*, vol. 75, no. 12, p. 125328, 2007.

(12)   C. Schaffner-Hamann, A. von Zelewsky, A. Barbieri, F. Barigelletti, G. Muller, J. P. Riehl, and A. Neels, "Diastereoselective formation of chiral tris-cyclometalated iridium (III) complexes: characterization and photophysical properties," *J. Am. Chem. Soc.*, vol. 126, no. 30, pp. 9339–9348, 2004.

(13)   J. Van Houten and R. J. Watts, "Temperature dependence of the photophysical and photochemical properties of the tris(2,2'-bipyridyl)ruthenium (II) ion in aqueous solution," *J. Am. Chem. Soc.*, vol. 98, no. 16, pp. 4853–4858, 1976.

(14)   T. J. Meyer, "Photochemistry of metal coordination complexes: metal to ligand charge transfer excited states," *Pure Appl. Chem.*, vol. 58, no. 9, pp. 1193–1206, 1986.

(15)   L. Yang, F. Okuda, K. Kobayashi, K. Nozaki, Y. Tanabe, Y. Ishii, and M.-a. Haga, "Syntheses and phosphorescent properties of blue emissive iridium complexes with tridentate pyrazolyl ligands," *Inorg. Chem.*, vol. 47, no. 16, pp. 7154–7165, 2008.

(16)   A. Islam, N. Ikeda, K. Nozaki, Y. Okamoto, B. Gholamkhass, A. Yoshimura, and T. Ohno, "Non-radiative processes of excited CT states of Ru(II) and Pt(II) compounds and excited dd states of Rh(III) compounds in the solid state and at higher temperatures," *Coord. Chem. Rev.*, vol. 171, pp. 355–363, 1998.

(17)   J. V. Caspar and T. J. Meyer, "Photochemistry of tris(2,2'-bipyridine) ruthenium (2+) ion (Ru(bpy)32+). Solvent effects," *J. Am. Chem. Soc.*, vol. 105, no. 17, pp. 5583–5590, 1983.

(18)   J.-L. Heully, F. Alary, and M. Boggio-Pasqua, "Spin-orbit effects on the photophysical properties of Ru(bpy)$_3$ $^{2+}$," *J. Chem. Phys.*, vol. 131, no. 18, p. 184308, 2009.

(19)   X. Zhou, P. L. Burn, and B. J. Powell, "Bond fission and non-radiative decay in iridium(III) complexes," *Inorg. Chem.*, vol. 55, no. 11, pp. 5266–5273, 2016.

(20)   J. Lee, H.-F. Chen, T. Batagoda, C. Coburn, P. I. Djurovich, M. E. Thompson, and S. R. Forrest, "Deep blue phosphorescent organic light-emitting diodes with very high brightness and efficiency," *Nat. mater.*, vol. 15, no. 1, p. 92, 2016.

(21)   T. Sajoto, P. I. Djurovich, A. Tamayo, M. Yousufuddin, R. Bau, M. E. Thompson, R. J. Holmes, and S. R. Forrest, "Blue and near-UV phosphorescence from iridium complexes with cyclometalated pyrazolyl or N-heterocyclic carbene ligands," *Inorg. Chem.*, vol. 44, no. 22, pp. 7992–8003, 2005.

(22)   P. Hohenberg and W. Kohn, "Inhomogeneous electron gas," *Phys. Rev.*, vol. 136, no. 3B, p. B864, 1964.

(23)   W. Kohn and L. J. Sham, "Self-consistent equations including exchange and correlation effects," *Phys. Rev.*, vol. 140, no. 4A, p. A1133, 1965.

(24)   P. J. Stephens, F. J. Devlin, C. F. Chabalowski, and M. J. Frisch, "Ab initio calculation of vibrational absorption and circular dichroism spectra using density functional force fields," *J. Phys. Chem.*, vol. 98, no. 45, pp. 11623–11627, 1994.

(25)   C. Lee, W. Yang, and R. G. Parr, "Development of the Colle-Salvetti correlation-energy formula into a functional of the electron density," *Phys. Rev. B*, vol. 37, no. 2, p. 785, 1988.

(26)   P. C. Hariharan and J. A. Pople, "The influence of polarization functions on

molecular orbital hydrogenation energies," *Theoret. Chim. Acta*, vol. 28, no. 3, pp. 213–222, 1973.

(27)   P. J. Hay and W. R. Wadt, "Ab initio effective core potentials for molecular calculations. Potentials for K to Au including the outermost core orbitals," *J. Chem. Phys.*, vol. 82, no. 1, pp. 299–310, 1985.

(28)   M. J. Frisch, G. W. Trucks, H. B. Schlegel, G. E. Scuseria, M. A. Robb, J. R. Cheeseman, G. Scalmani, V. Barone, B. Mennucci, G. A. Petersson, H. Nakatsuji, M. Caricato, X. Li, H. P. Hratchian, A. F. Izmaylov, J. Bloino, G. Zheng, J. L. Sonnenberg, M. Hada, M. Ehara, K. Toyota, R. Fukuda, J. Hasegawa, M. Ishida, T. Nakajima, Y. Honda, O. Kitao, H. Nakai, T. Vreven, J. A. Montgomery, Jr., J. E. Peralta, F. Ogliaro, M. Bearpark, J. J. Heyd, E. Brothers, K. N. Kudin, V. N. Staroverov, R. Kobayashi, J. Normand, K. Raghavachari, A. Rendell, J. C. Burant, S. S. Iyengar, J. Tomasi, M. Cossi, N. Rega, J. M. Millam, M. Klene, J. E. Knox, J. B. Cross, V. Bakken, C. Adamo, J. Jaramillo, R. Gomperts, R. E. Stratmann, O. Yazyev, A. J. Austin, R. Cammi, C. Pomelli, J. W. Ochterski, R. L. Martin, K. Morokuma, V. G. Zakrzewski, G. A. Voth, P. Salvador, J. J. Dannenberg, S. Dapprich, A. D. Daniels, O. Farkas, J. B. Foresman, J. V. Ortiz, J. Cioslowski, and D. J. Fox, "Gaussian 09, revision e.01," Gaussian Inc., Wallingford CT, 2009.

(29)   A. S. Menon and L. Radom, "Consequences of spin contamination in unrestricted calculations on open-shell species: Effect of Hartree-Fock and Møller-Plesset contributions in hybrid and double-hybrid density functional theory approaches," *J. Phys. Chem. A*, vol. 112, no. 50, pp. 13225–13230, 2008.

(30)   G. B. Bacskay, "A quadratically convergent Hartree–Fock (QC-SCF) method. Application to closed shell systems," *Chem. Phys.*, vol. 61, no. 3, pp. 385–404, 1981.

(31)   F. Wang and T. Ziegler, "A simplified relativistic time-dependent density-functional theory formalism for the calculations of excitation energies including spin-orbit coupling effect," *J. Chem. Phys.*, vol. 123, no. 15, p. 154102, 2005.

(32)   M. E. Casida, "Time-dependent density functional response theory for molecules," in *Recent advances in density functional methods*, D. P. Chong, Ed. World Scientific, 1995, vol. 1, p. 155.

(33)   M. E. Casida, "Time-dependent density-functional theory for molecules and molecular solids," *J. Mol. Struct. THEOCHEM*, vol. 914, no. 1, pp. 3–18, 2009.

(34)   E. Runge and E. K. U. Gross, "Density-functional theory for time-dependent systems," *Phys. Rev. Lett.*, vol. 52, no. 12, p. 997, 1984.

(35)   C. Chang, M. Pelissier, and P. Durand, "Regular two-component Pauli-like effective Hamiltonians in Dirac theory," *Phys. Scr.*, vol. 34, no. 5, pp. 394–404, 1986.

(36)   E. Van Lenthe, E. J. Baerends, and J. G. Snijders, "Relativistic total energy using regular approximations," *J. Chem. Phys.*, vol. 101, no. 11, pp. 9783–9792, 1994.

(37)   S. J. Strickler and R. A. Berg, "Relationship between absorption intensity and fluorescence lifetime of molecules," *J. Chem. Phys.*, vol. 37, no. 4, pp. 814–822,

1962.

(38)   K. Nozaki, "Theoretical studies on photophysical properties and mechanism of phosphorescence in [fac-Ir(2-phenylpyridine)$_3$]," *J. Chin. Chem. Soc.*, vol. 53, no. 1, pp. 101–112, 2006.

(39)   E. J. Baerends, T. Ziegler, A. J. Atkins, J. Autschbach, D. Bashford, O. Baseggio, A. Bérces, F. M. Bickelhaupt, C. Bo, P. M. Boerritger, L. Cavallo, C. Daul, D. P. Chong, D. V. Chulhai, L. Deng, R. M. Dickson, J. M. Dieterich, D. E. Ellis, M. van Faassen, A. Ghysels, A. Giammona, S. J. A. van Gisbergen, A. Goez, A. W. Götz, S. Gusarov, F. E. Harris, P. van den Hoek, Z. Hu, C. R. Jacob, H. Jacobsen, L. Jensen, L. Joubert, J. W. Kaminski, G. van Kessel, C. König, F. Kootstra, A. Kovalenko, M. Krykunov, E. van Lenthe, D. A. McCormack, A. Michalak, M. Mitoraj, S. M. Morton, J. Neugebauer, V. P. Nicu, L. Noodleman, V. P. Osinga, S. Patchkovskii, M. Pavanello, C. A. Peeples, P. H. T. Philipsen, D. Post, C. C. Pye, H. Ramanantoanina, P. Ramos, W. Ravenek, J. I. Rodríguez, P. Ros, R. Rüger, P. R. T. Schipper, D. Schlüns, H. van Schoot, G. Schreckenbach, J. S. Seldenthuis, M. Seth, J. G. Snijders, M. Solà, S. M., M. Swart, D. Swerhone, G. te Velde, V. Tognetti, P. Vernooijs, L. Versluis, L. Visscher, O. Visser, F. Wang, T. A. Wesolowski, E. M. van Wezenbeek, G. Wiesenekker, S. K. Wolff, T. K. Woo, and A. L. Yakovlev, "ADF2017, SCM, Theoretical Chemistry, Vrije Universiteit, Amsterdam, The Netherlands, https://www.scm.com."

(40)   B. J. Powell, "Theories of phosphorescence in organo-transition metal complexes – From relativistic effects to simple models and design principles for organic light-emitting diodes," *Coord. Chem. Rev.*, vol. 295, pp. 46–79, 2015.

(41)   B. J. Powell, "Conservation laws, radiative decay rates, and excited state localization in organometallic complexes with strong spin-orbit coupling," *Sci. Rep.*, vol. 5, p. 10815, 2015.

(42)   E. Van Lenthe and E. J. Baerends, "Optimized Slater-type basis sets for the elements 1–118," *J. Comput. Chem.*, vol. 24, no. 9, pp. 1142–1156, 2003.

(43)   D. P. Chong, "Augmenting basis set for time-dependent density functional theory calculation of excitation energies: Slater-type orbitals for hydrogen to krypton," *Mol. Phys.*, vol. 103, no. 6-8, pp. 749–761, 2005.

(44)   A. Dreuw, J. L. Weisman, and M. Head-Gordon, "Long-range charge-transfer excited states in time-dependent density functional theory require non-local exchange," *J. Chem. Phys.*, vol. 119, no. 6, pp. 2943–2946, 2003.

(45)   A. Dreuw and M. Head-Gordon, "Failure of time-dependent density functional theory for long-range charge-transfer excited states: The zincbacteriochlorin-bacteriochlorin and bacteriochlorophyll-spheroidene complexes," *J. Am. Chem. Soc.*, vol. 126, no. 12, pp. 4007–4016, 2004.

(46)   D. J. Tozer, "Relationship between long-range charge-transfer excitation energy error and integer discontinuity in Kohn–Sham theory," *J. Chem. Phys.*, vol. 119, no. 24, pp. 12697–12699, 2003.

(47)   D. J. Tozer, R. D. Amos, N. C. Handy, B. O. Roos, and L. Serrano-Andres, "Does density functional theory contribute to the understanding of excited states of unsaturated organic compounds?" *Mol. Phys.*, vol. 97, no. 7, pp. 859–868, 1999.

(48)   A. R. G. Smith, P. L. Burn, and B. J. Powell, "Exact exchange and the density functional theory of metal-to-ligand charge-transfer in fac-ir(ppy)$_3$," *Org. Electron.*, vol. 33, pp. 110–115, 2016.

(49)   A. R. G. Smith, M. J. Riley, P. L. Burn, I. R. Gentle, S.-C. Lo, and B. J. Powell, "Effects of fluorination on iridium(III) complex phosphorescence: magnetic circular dichroism and relativistic time-dependent density functional theory," *Inorg. Chem.*, vol. 51, no. 5, pp. 2821–2831, 2012.

For Table of Contents Only

We investigated the non-radiative pathways and the stability of a family of Ir(III) complexes based on *N*-heterocyclic carbene (NHC) ligands. Specifically, we identified the non-radiative decay pathway with the lowest barrier energy of these complexes as the elongation of an Ir-C (NHC) bond by the computation of the triplet potential energy surface. We also discussed how ligand substitution and structural isomerization affect the photoluminescence efficiency and the stability of these complexes.